Hindawi
Advances in Civil Engineering
Volume 2023, Article ID 5104132, 14 pages
https://doi.org/10.1155/2023/5104132

Research Article

Study on the Dynamic Response of Composite Box Girder Bridges with Corrugated Steel Webs

Ya-Na Mao,[1,2] Chi Ma,[1] Shi-Zhong Liu,[1] and Li-Yuan Li[1]

[1]*College of Civil Engineering, Lanzhou Jiaotong University, Lanzhou 730070, China*
[2]*Gansu Road and Bridge Highway Investment Co Ltd, Lanzhou, Gansu 730030, China*

Correspondence should be addressed to Chi Ma; 308329771@qq.com

Received 14 June 2022; Revised 30 November 2022; Accepted 29 March 2023; Published 27 April 2023

Academic Editor: Khaled Ghaedi

To more accurately consider the dynamic response of composite box girder bridges with corrugated steel webs under the effect of live loads, based on the theory of vehicle-bridge coupled vibration, a refined finite element model of vehicle-bridge coupled vibration analysis for composite box girders was established. The advanced dynamic response analysis of composite box girders with corrugated steel webs and traditional concrete box girders with 30 m single boxes and single cells, as well as with 50 m single boxes and multiple cells, was carried out. The research revealed that the natural vibration frequency of the composite box girder with corrugated steel webs is lower than that of the corresponding concrete box girder. When the bridge deck condition is poor, the dynamic impact coefficient of the composite box girder is much larger than that of the concrete box girder. When the bridge deck is in poor condition, the dynamic impact response is significantly enhanced, and the difference is significantly compared with that when the bridge deck is in good condition, which is greater than three times and even six times at the maximum. Both the difference in the vehicle model and the change in the vehicle speed influence the dynamic impact coefficient of the composite box girder.

1. Introduction

For a composite box girder bridge with corrugated steel webs, replacing a concrete web with a steel web in a composite box girder with corrugated steel webs can effectively reduce the weight of the structure, which will inevitably lead to an increase in the ratio of live load to dead load. Therefore, the dynamic response generated by the live load will become more obvious. Based on the energy variation principle, Zhang et al. [1] comprehensively considered the effects of shear lag, fold, shear deformation, and moment of inertia, derived the dynamic control differential equation and boundary conditions of the continuous composite box girder bridge with corrugated steel webs, and analysed the natural vibration characteristics of the continuous composite box girder bridge with corrugated steel webs in combination with model tests and finite element numerical simulations. Chen et al. [2] constructed a three-span prestressed concrete and continuous corrugated steel web test beam and carried out a dynamic test on it. The authors also carried out a dynamic test on a real bridge and compared the test results of the test beam and the real bridge with the finite element results. Zheng et al. [3, 4] constructed two corresponding test beams, compared the dynamic characteristics of the two beams with a combination of model tests and finite element numerical simulations, and analysed the influence of external prestress and its parameter changes on the natural frequency of a continuous box girder with corrugated steel webs. Based on box girder vibration theory, Wang et al. [5] proposed a method to calculate the natural frequency of a new composite box girder with corrugated steel webs under the action of time-varying temperature, which considered the slip effect. The proposed method was verified by finite element simulation and model test beam actual measurement. Wei et al. [6, 7] obtained the formula of vertical fundamental frequency correction for a continuous composite box girder with variable section corrugated steel webs by model testing and ANSYS finite element simulation

analysis and obtained the partial and integral impact coefficients of the composite box girder with corrugated steel webs by establishing the coupling vibration equation of the vehicle and bridge with a simply supported composite box girder. The current Chinese General Specification for Highway Bridge and Culvert Design (JTG D60-2015) [8] provides a formula for the dynamic impact coefficient based on the natural vibration frequency of the bridge. From the analysis of the natural vibration frequency of corrugated steel webs, due to the impact of the shear deformation of steel webs, the natural vibration frequency of the composite box girder should be multiplied by the reduction coefficient a_{2n} in the primary beam result [9]. The calculation formula of the impact coefficient provided in the specification is based on the impact coefficient samples of more than 6,600 concrete bridges with 6 m–45 m spans and is obtained by using the method of mathematical statistics and appropriate correction. It is necessary to further verify whether the impact coefficient formula is suitable for composite box girders with corrugated steel webs. Although Chinese bridge codes do not clearly list influence factors such as the deck condition, vehicle type, and speed for the impact coefficient of a bridge, some analyses have indicated that these factors have a certain influence on the dynamic impact coefficient [10–12]. Thus, these factors need to be analysed to provide a reference for the dynamic load test evaluation of this type of bridge in service.

In summary, to more accurately consider the dynamic response of the composite box girder with corrugated steel webs under the effect of live load and to properly analyse corrugated steel webs composite box girders in service, the dynamic impact coefficient of this composite box girder should be investigated.

2. Estimation and Analysis of the Dynamic Impact Coefficient of the Composite Box Girder

2.1. Domestic Highway Bridge Code. The Chinese General Specification for Design of Highway Bridges and Culverts (JTG D60-2015) stipulates that based on the research results of road bridge reliability, the impact coefficient of bridge structures is calculated by structural base frequency. The formula for calculating the impact coefficient μ is presented as follows:

$$\mu = \begin{cases} 0.005, & f < 1.5Hz, \\ 0.1767\mathrm{In}\, f - 0.0157, & 1.5Hz \le f \le 14Hz, \\ 0.45, & f > 14Hz. \end{cases} \quad (1)$$

In the formula, f refers to the fundamental frequency of a structure (Hz). The specification provides the frequency estimation formula for the following simply supported beam:

$$f = \frac{\pi}{2l^2}\sqrt{\frac{EI_c}{m_c}}, \quad (2)$$

where l is the calculated span of the structure; I_c is the moment of inertia of the midspan section of the structure; m_c is the mass per unit length at the middle span of the structure, namely, $m_c = G/g$; G is the gravity of the structure per linear metre at the midspan of the structure; and g is the acceleration of gravity.

By comparing formula (2) with the calculation expression of the fundamental frequency of the composite box girder with corrugated steel webs, we know that due to the shear deformation of the corrugated steel web, the natural frequency of the composite box girder in formula (2) needs to be multiplied by the reduction factor a_{2n}. The impact coefficient in the article interpretation code is based on the actual measurement results of the concrete box girder bridge and is obtained through mathematical statistical analysis. However, the applicability of the composite box girder bridge with corrugated steel webs should be further analysed.

The impact coefficient in the specification interpretation is based on the measured results of the concrete box girder bridge, which is derived from the statistical analysis, and the applicability of the composite box girder bridge with corrugated steel webs should be further analysed.

2.2. International Highway Bridge Code. The 2012 version of the AASHTO bridge design specification is described in terms of dynamic load tolerance (DLA), and its value depends on the limit state and component type. Presently, the impact coefficient used by the US Code for strength assessment of active bridges is determined according to the level of pavement roughness, and the dynamic impact coefficient of the limit assessment of active bridges is specified to be 0.33 [13, 14].

The impact coefficient defined in the Japanese JRA (1996 edition) Highway Bridge Design Code is also a function of the bridge span, but it distinguishes bridges of different material types. The expressions of impact coefficients corresponding to vehicle loads are the same, while there are obvious differences in lane loads [15].

The Canadian 1983 edition of the Highway Bridge Design Code stipulates that the calculation formula of the impact coefficient μ of a bridge is similar to the 2004 edition of the Chinese Highway Bridge Design Code; both are based on the first-order flexural natural vibration frequency f_1 of a bridge. The 1991 edition of the Canadian Highway Bridge Design Code introduced the relationship between the number of axles and the impact coefficient, with a similar relationship specified in the most recent edition of the code. The main difference is that the impact coefficient μ at the bridge joint is 0.5 [16, 17].

By summarizing the simplified calculation formulas of impact coefficients in design codes of highway bridges worldwide, we obtained the following findings: (1) each country's highway and bridge design codes have different requirements on automobile impact coefficients; (2) different codes define the impact coefficient as the expression of different bridge parameters, such as bridge span, bridge natural frequency, and vehicle or lane load type; and (3) the

national codes do not clearly indicate the type of dynamic response of the bridge corresponding to the impact coefficient, and the codes have limited influence factors for simplicity and utility.

2.3. Comparative Analysis of the Dynamic Response of the Composite Box Girder. Many international codes consider the impact of different types of bridges, especially steel bridges and concrete bridges, on dynamic impact. Chinese codes do not subdivide bridge types into steel bridges and concrete bridges. Presently, there is no specification that gives special consideration to the dynamic impact response of the special type of bridge with a corrugated steel web composite box girder. Consequently, composite box girder bridges with corrugated steel webs were analysed and compared with concrete box girder bridges, and samples of single box, single cell, and single box twin cell girders were selected for comparison.

2.3.1. Single Box, Single Cell Composite Box Girder with Corrugated Steel Webs. A section of a composite box girder with corrugated steel webs, as shown in Figure 1(a), is selected, and the span combination of a 1×30 m simply supported beam and a 2×30 m continuous box girder is employed. The elastic modulus of the flange plate is 34.5 GPa, and Poisson's ratio is 0.2. The elastic modulus of the steel is 206 GPa, and Poisson's ratio is 0.3. The characteristics of the steel web are shown in Figure 1(b). The steel web is replaced by a concrete web for comparison and analysis, and the cross-sectional parameters are shown in Figure 1(c). The concrete material properties are identical to the material properties of the corrugated steel web combination box.

The spatial finite element model of the abovementioned composite box girder with corrugated steel webs and concrete box girder was established using ANSYS spatial finite element software to calculate the natural frequency of the model. The natural frequencies of composite box girders with corrugated steel webs and concrete box girders were calculated by the general specification of highway bridges and culverts and the method of [12], respectively. The results are listed in Table 1.

2.3.2. Single Box, Twin Cell Composite Box Girder with Corrugated Steel Webs. A section of a composite box girder with corrugated steel webs, as shown in Figures 2 and 2(a), with a span of 1×50 m is selected. The material characteristics are the same as those of the single box, single-cell composite box girder mentioned above. The characteristics of the steel web are shown in Figure 2(b). The cross-sectional parameters of the concrete box girder used for comparison are shown in Figure 2(c). The box girder deflection, natural vibration frequency calculated by highway specification 89 is shown in Table 2.

By comparing the frequencies in Table 1, we obtained the following findings: (1) The analytical results in this article show agreement with the ANSYS solid finite element results. Tables 1 and 2 show that after the corrugated steel webs are replaced with ordinary concrete webs, the difference between the calculated low-order frequencies is small. However, as the frequency order increases, the difference between the two frequency values increases, and the frequency of the composite box girder with corrugated steel webs is lower than that of the concrete box beams.

The provisions of the domestic and international codes for the dynamic impact coefficient of bridges are mostly calculated based on the span or frequency, with the exception of distinguishing the material type. Based on an analysis of the natural frequency of corrugated steel webs and the corresponding concrete box girder, the dynamic impact coefficient of composite box girder bridges with corrugated steel webs is calculated according to domestic and international specifications, as shown in Table 3.

As shown in Table 3, according to the different impact coefficients calculated by the domestic and international codes, the Canadian code has the largest value, the Chinese 89 edition code has the smallest value, and the Chinese code, 15th edition, is relatively similar to the American and Japanese codes. In addition, note that the Chinese code, 15th edition, gives frequency estimation formulas for simply supported and continuous beams. The impact coefficient of a 30 m span, simply supported beam calculated according to the relevant formula is 0.257, the impact coefficient of the midsection of the continuous beam span is 0.314, and the impact coefficient of the fulcrum is 0.412.

3. Numerical Simulation of the Dynamic Response of the Composite Box Girder

According to the frequency of the composite box girder with corrugated steel webs and the corresponding concrete box girder and the specifications on the dynamic impact coefficient, when the span and frequency are equivalent, the dynamic impact coefficients of the composite box girder with corrugated steel webs and the concrete box girder are similar. However, the actual situation needs further comparison and analysis. The dynamic test of a bridge is relatively difficult to implement due to factors such as the external environment, the use of the bridge, and costs. Presently, with the rapid development of computer simulation and extensive theoretical research on vehicle-bridge coupling analysis, vibration and shock analysis of bridges can be achieved by numerical simulation.

3.1. Numerical Simulation of Cars. According to relevant research and the provisions of the aforementioned US and Canadian codes, the parameters of vehicles, such as their types, axles, axle load, and vehicle fundamental frequency, have different impacts on the dynamic impact coefficient of bridges. The selected vehicles are the two- and three-axis vehicle models commonly employed by scholars worldwide to analyse the coupling vibration of the axle [1, 2].

3.2. Pavement Smoothness Simulation. Pavement smoothness is an important source of excitation in vehicle-bridge coupled vibration analysis, and it has a large randomness.

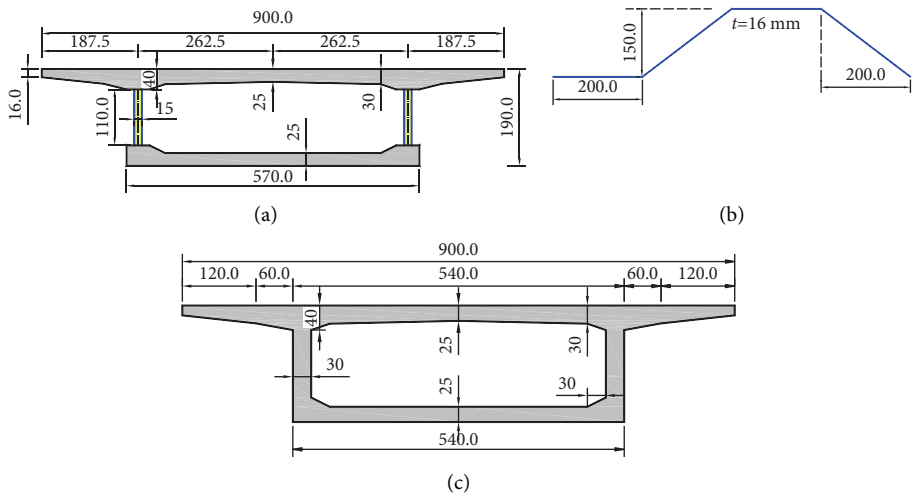

Figure 1: Cross-sectional diagram of the box girder: (a) section of the composite box girder with corrugated steel webs (cm), (b) detail of the corrugated steel web (mm), and (c) reinforced concrete box girder section (cm).

Table 1: Box beam natural frequencies calculated by different methods (unit: Hz).

Frequency order	Calculation method	Simply supported beam		2-Span continuous beam	
		Composite box girder	Concrete box girder	Composite box girder	Concrete box girder
1	Analytical method	4.452	4.479	4.452	4.479
	ANSYS entity	4.396	4.397	4.484	4.491
2	Analytical method	14.637	15.899	6.305	6.506
	ANSYS entity	13.217	14.453	6.087	6.569
3	Analytical method	24.099	30.763	14.637	15.899
	ANSYS entity	20.204	22.075	13.513	14.883

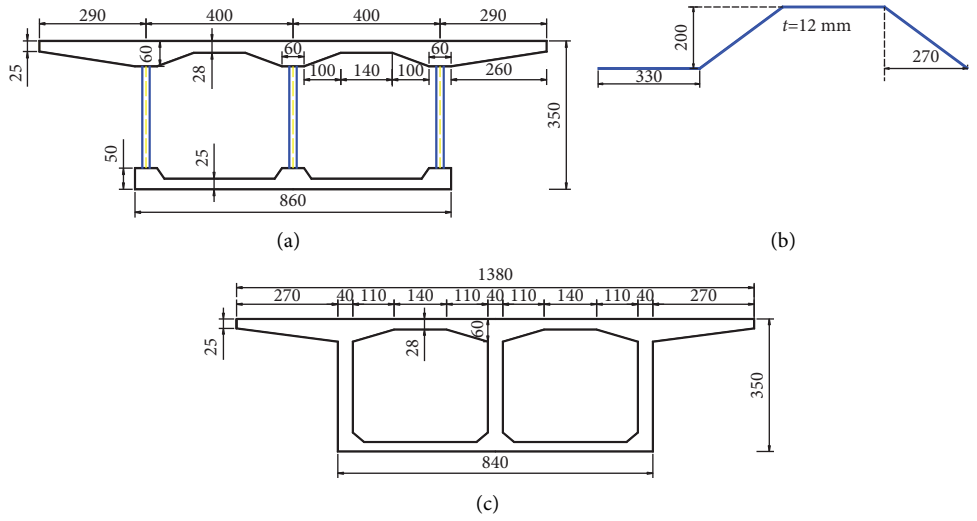

Figure 2: Schematic of the box girder section: (a) section of the composite box girder with corrugated steel webs (cm), (b) detail of the corrugated steel web (mm), and (c) reinforced concrete box girder section (cm).

When numerically simulating pavement smoothness, the method of series is usually applied to generate the pavement flatness curve that meets the power spectrum function. The formula of the power spectral density function of pavement smoothness is as follows [18]:

$$\varphi(n) = \varphi(n_0)\left(\frac{n}{n_0}\right)^{-2}, \quad (n_1 < n < n_2), \tag{3}$$

where $\varphi(n_0)$ is the road surface smoothness coefficient corresponding to the standard spatial frequency; n and n_0 are

Table 2: Comparison of the natural frequency of the 50 m box girder (unit: Hz).

Frequency order	Composite box girder with corrugated steel webs	Concrete box girder
1	2.975	2.971
2	9.464	11.079
3	18.785	22.583

the spatial frequency and standard spatial frequency, respectively; and n_1 and n_2 are the indices of the road power spectrum in the low frequency band and high frequency band, respectively.

The formula for generating the road surface flatness curve by the series method is as follows:

$$r(x) = \sum_{k=1}^{N} \sqrt{2\varphi(n_k)\Delta n}\cos(2\pi n_k x + \theta_k), \tag{4}$$

where x is the coordinate along the bridge axis; n_k, Δn, and N are the spatial frequency sampling point, sampling interval, and sampling number, respectively; and θ_k is the random phase angle in the interval $(0, 2\pi)$.

The road surface roughness is divided into five levels according to the International Organization for Standardization: very good, good, normal, poor, and very poor [19]. As the road surface smoothness curve generated according to the series method has large randomness, it masks the essential law of the dynamic impact coefficient. The solution is to use multiple road roughnesses for vehicle-bridge coupling vibration calculations to obtain multiple dynamic response values of the bridge structure, and then to calculate the average value to reduce the randomness of pavement flatness.

3.3. Solution of Vehicle-Bridge Coupling Vibration Equation. There have been many relevant theoretical studies on the dynamic coupling vibration equation of vehicles and bridges [20–23]. According to the relevant research, the dynamic equations of the respective systems of vehicles and bridges are shown in the following equations:

$$\mathbf{M}_v\ddot{\mathbf{d}}_v + \mathbf{C}_v\dot{\mathbf{d}}_v + \mathbf{K}_v\mathbf{d}_v = \mathbf{F}_{vg}\mathbf{F}_{vr}, \tag{5}$$

$$\mathbf{M}_b\ddot{\mathbf{d}}_b + \mathbf{C}_b\dot{\mathbf{d}}_b + \mathbf{K}_b\mathbf{d}_b = \mathbf{F}_{br}, \tag{6}$$

where $\mathbf{M}$, $\mathbf{C}$, and $\mathbf{K}$ are the mass, damping, and stiffness matrices, respectively; d is the system displacement vector; subscripts $v$and b represent vehicles and bridges, respectively; $\mathbf{F}_{vg}$ is the equivalent node load sequence vector caused by a vehicle's own weight; and $\mathbf{F}_{vr}$ and $\mathbf{F}_{br}$ are the interaction forces between the bridge and the vehicle system.

According to the contact relationship between the wheel and the bridge deck and the contact force between them when a vehicle crosses the bridge, the relationship of formulas (5) and (6) is established, and the important expression of the axle-coupled vibration is formed as follows:

$$\begin{bmatrix} \mathbf{M}_b & \\ & \mathbf{M}_v \end{bmatrix}\begin{Bmatrix} \mathbf{d}_b \\ \mathbf{d}_v \end{Bmatrix} + \begin{bmatrix} \mathbf{C}_b + \mathbf{C}_{b-b} & \mathbf{C}_{b-v} \\ \mathbf{C}_{v-b} & \mathbf{C}_v \end{bmatrix}\begin{Bmatrix} \dot{\mathbf{d}}_b \\ \dot{\mathbf{d}}_v \end{Bmatrix} + \begin{bmatrix} \mathbf{K}_b + \mathbf{K}_{b-b} & \mathbf{K}_{b-v} \\ \mathbf{K}_{v-b} & \mathbf{K}_v \end{bmatrix}\begin{Bmatrix} \mathbf{d}_b \\ \mathbf{d}_v \end{Bmatrix} = \begin{Bmatrix} \mathbf{F}_{b-v} \\ \mathbf{F}_{v-r} + \mathbf{F}_{vg} \end{Bmatrix}, \tag{7}$$

where $\mathbf{C}_{b\text{-}b}$, $\mathbf{C}_{b\text{-}v}$, $\mathbf{C}_{v\text{-}b}$, $\mathbf{K}_{b\text{-}b}$, $\mathbf{K}_{b\text{-}v}$, $\mathbf{K}_{v\text{-}b}$, $\mathbf{F}_{b\text{-}r}$, and $\mathbf{F}_{v\text{-}r}$ are additional terms resulting from the axle-bridge coupling effect.

For the solution method of vehicle-bridge coupled vibration expression (7), the direct integration method or modal synthesis method is generally adopted [16]. Since this article will establish a spatial solid model of corrugated steel web composite box girders and the corresponding concrete box beams, there will be many nodes and elements. Thus, this article adopts the modal synthesis method, which effectively reduces the calculation workload for more complicated bridges and obtains a more accurate numerical solution. The specific simulation method is described as follows: first, ANSYS spatial finite element software is used to establish a solid finite element model of the composite box girder and the corresponding concrete box girder, to calculate its natural frequency and vibration mode, and to extract the corresponding modal matrix. Then, MATLAB software is used to compile the fourth-order Runge–Kutta method and import the modal matrix of the bridge to solve equation (7) to obtain the dynamic response of the bridge.

4. Analysis of the Dynamic Shock Response of the Composite Box Girder

To analyse the dynamic impact coefficient of the composite box girder, the above example is used, and the test section is the midspan section. The arrangement of measuring points on the composite box girder is shown in Figure 3, and the measuring points of the concrete box girder are the same as those of the composite box girder. To verify the correctness of the vehicle-bridge coupling program in this article, by disregarding the pavement state, reducing the vehicle speed to 1 m/s and setting the load step to 0.002 s, the vertical displacement generated by a vehicle passing the bridge and the analysis results of the static force of ANSYS are compared. The selected measuring points are 8 and 9, as shown in Figures 4(a) and 4(b), and the comparison results are shown in Figure 4.

A comparative analysis of Figure 4 reveals that the error between the simulated static analysis results of the MATLAB program in this article and the static analysis results of the ANSYS solid model is very small (within 5%), which shows

Table 3: Dynamic impact coefficient of composite box girder with corrugated steel webs.

Span (m)	Material type	CHN 89 edition specification	CHN 15 edition specification	USA 92 edition specification	JPN 96 edition specification	CAN specification
30	Concrete bridge	0.113	0.249	0.224	0.250	0.400
	Steel bridge	0.222	0.249	0.224	0.250	0.400
50	Concrete bridge	0.000	0.177	0.173	0.200	0.400
	Steel bridge	0.171	0.177	0.173	0.200	0.400

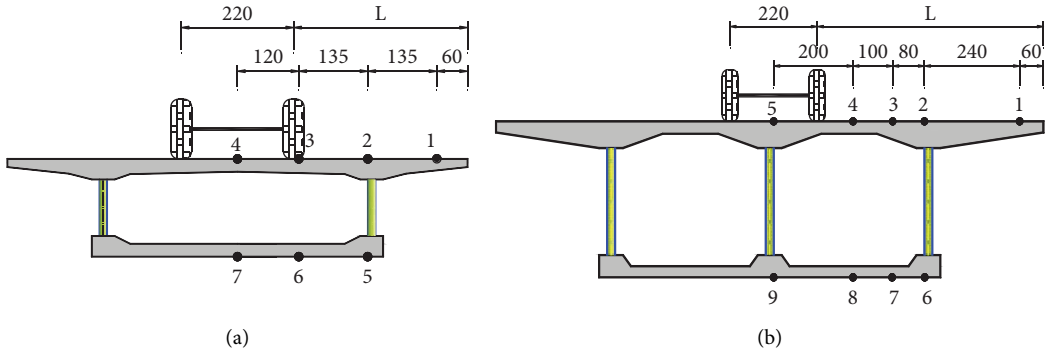

Figure 3: Schematic layout of the measuring points of the composite box girder: (a) single box, single cell measuring point arrangement (cm) and (b) single box, twin cell measuring point arrangement (cm).

that the procedure of this article is correct and verifies that the modal order is taken to meet the calculation accuracy requirements.

4.1. Analysis of the Deflection Impact Coefficient of Composite Box Girders with Different Cross-Sections. In the calculation of the vehicle-bridge coupling analysis program, considering that the pavement state is divided into five levels in the International Organization for Standardization, the relevant specifications also clearly stated that the pavement condition has a greater impact on the impact coefficient. When the vehicle is travelling at a speed of 5 m/s, the time-history curve of the midspan deflection of the 30 m simply supported composite box girder with corrugated steel webs under different bridge deck conditions is shown in Figure 5. Figure 5(b) clearly shows that the dynamic shock response is significantly enhanced when the bridge deck is in poor condition and is significantly different when the bridge deck is in good condition.

To compare the difference between the impact coefficient of the composite box girder and the corresponding concrete box girder at the same frequency, the 30 m simple-supported composite box girder of sample 1 was selected as an example, using the vehicle-bridge coupling program in this article to calculate a vehicle speed of 5 m/s. The calculation results are shown in Tables 4 and 5. Figure 6 shows a comparison of the average value of the dynamic impact coefficient for each measuring point under different bridge deck conditions. Figure 7 shows the dynamic impact coefficient for each measuring point of the roof under different bridge deck conditions.

A comparison of Tables 4 and 5 shows the following findings: (1) The condition of the bridge deck has a great influence on the dynamic impact coefficient. When the condition of the bridge deck ranges from normal to very poor, the calculated dynamic impact coefficient is greater than the dynamic impact coefficient calculated in Table 3 according to the bridge specifications, which indicates that the dynamic impact coefficient given by the current Chinese bridge codes is applicable to the bridge deck in good or better condition. (2) When the bridge deck condition is very good and good, the dynamic impact coefficient of the composite box girder with corrugated steel webs is similar to that of the ordinary concrete box girder, which suggests that when the road surface is in good condition, the dynamic impact coefficient of an ordinary concrete box girder can be used to analyse the corrugated steel web composite box girder by simply changing the web. (3) When the condition of the bridge deck ranges from normal to poor, the average dynamic impact coefficient of the composite box girder is larger than that of the general concrete box girder (as shown in Figure 6), and as the condition of the bridge deck deteriorates, the increasing trend becomes more obvious. When the bridge deck is in poor condition, the impact coefficient of the composite box girder is increased by approximately 70% compared to the concrete box girder. (4) The dynamic impact coefficient of the two types of box girders will gradually increase from the centroid to the outside along the horizontal axis (as shown in Figure 7).

4.2. Analysis of the Strain Impact Coefficient of Vehicles Driving in Different Positions. After analysing the deflection impact coefficient of the composite box girder and the corresponding concrete box girder, determining whether the strain impact coefficient is consistent with the deflection impact coefficient value needs further analysis. The 50 m simply supported composite box girder with corrugated steel webs of sample 2 was selected as the research object. The

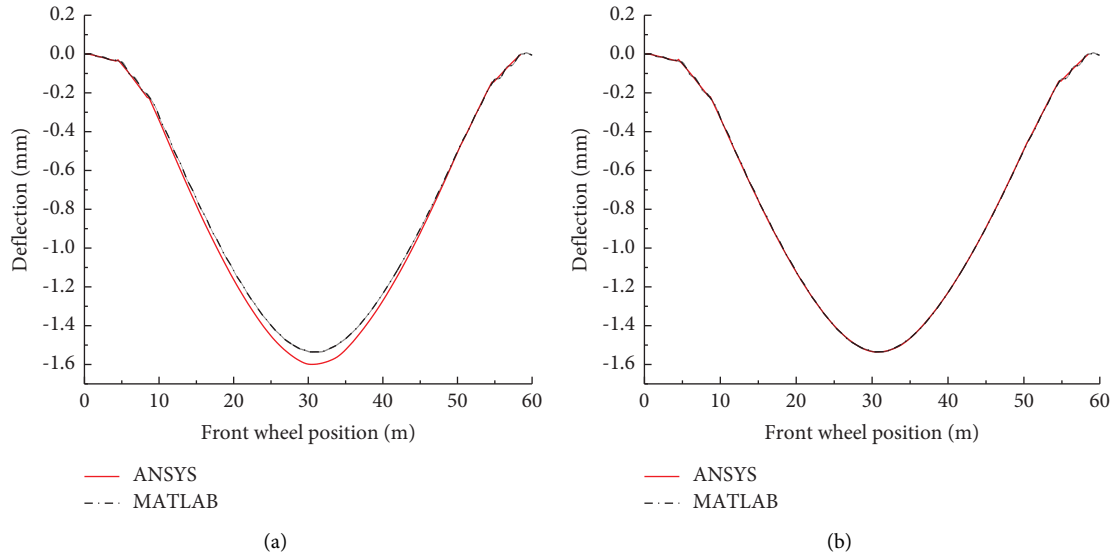

Figure 4: Comparison of deflection time history of 50 m composite box girder midspan measurement points in ANSYS and MATLAB. (a) Measuring point 8. (b) Measuring point 9.

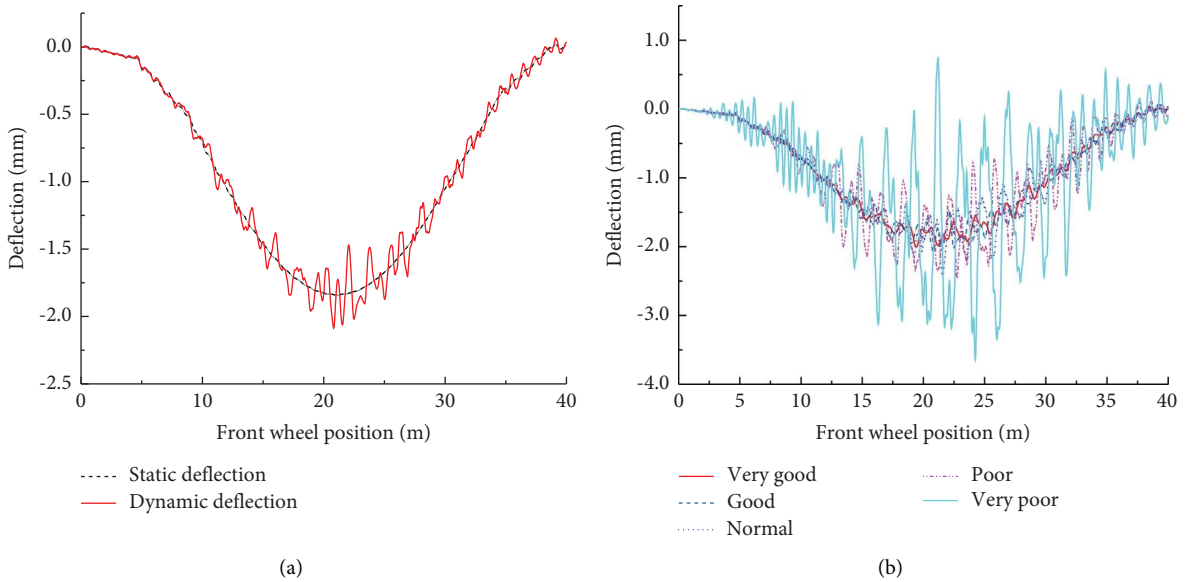

Figure 5: Deflection time-history curve of the midspan cross-section of the 30 m simply supported composite box girder under different road conditions. (a) Typical dynamic deflection time history curve (the bridge deck is in good condition). (b) Time point curve of measuring point 5 under different bridge conditions.

Table 4: Deflection dynamic impact coefficient of the 30 m simply supported composite box girder.

Measuring point	Very good	Good	Normal	Poor	Very poor
1	0.069	0.134	0.328	0.639	2.032
2	0.059	0.112	0.273	0.555	1.768
3	0.052	0.096	0.231	0.486	1.546
4	0.047	0.084	0.203	0.449	1.369
5	0.060	0.113	0.274	0.557	1.775
6	0.056	0.104	0.254	0.517	1.611
7	0.052	0.092	0.226	0.487	1.413

Table 5: Deflection dynamic impact coefficient of the 30 m simply supported concrete box girder.

Measuring point	Very good	Good	Normal	Poor	Very poor
1	0.067	0.139	0.259	0.603	1.087
2	0.061	0.127	0.230	0.538	0.986
3	0.055	0.114	0.204	0.471	0.875
4	0.049	0.104	0.186	0.422	0.794
5	0.061	0.128	0.231	0.538	0.986
6	0.057	0.122	0.215	0.487	0.918
7	0.053	0.113	0.195	0.444	0.828

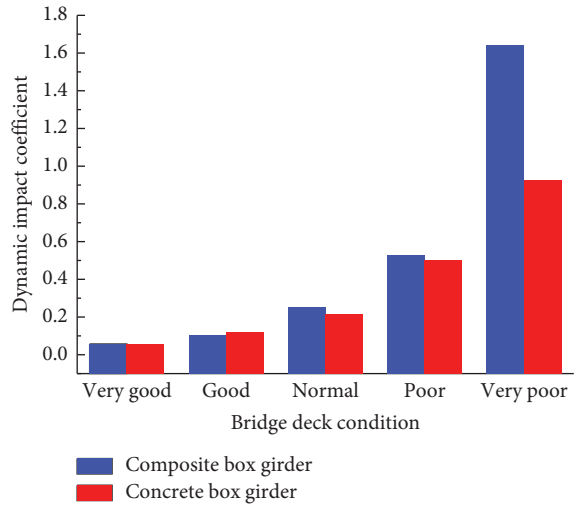

Figure 6: Comparison of the dynamic impact coefficients of the two box girders under different bridge deck conditions.

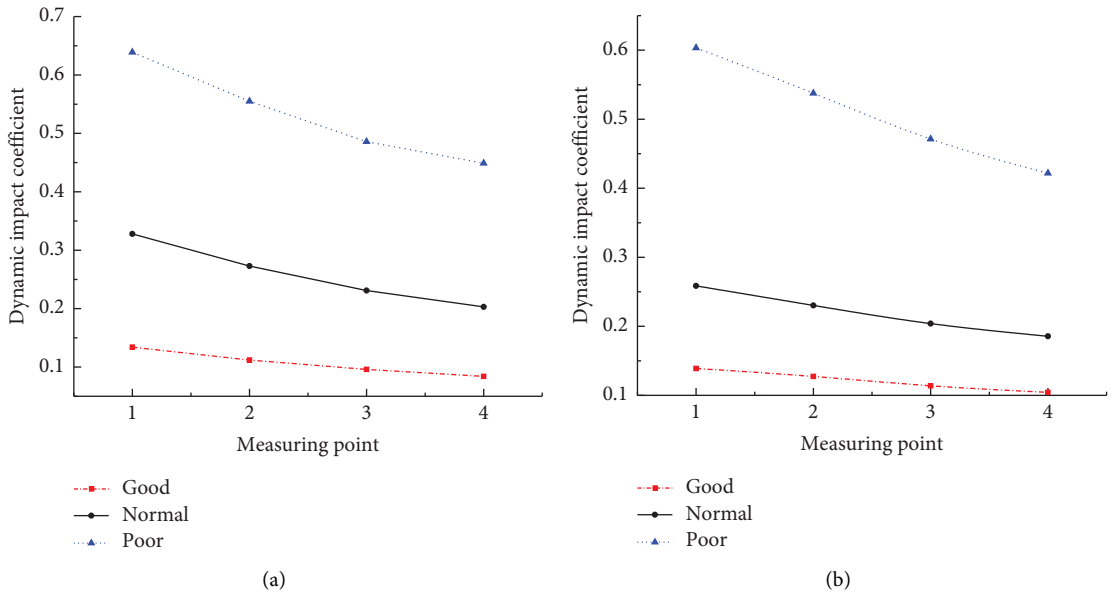

Figure 7: Dynamic impact coefficient of each measuring point of the roof under different road conditions: (a) composite box girder and (b) concrete box girder.

typical dynamic strain time-history curve of the 50 m composite box girder midspan floor is shown in Figure 8. The vehicle is driven with two loads, medium load ($L = 5.8$ m) and partial load ($L = 1$ m), and the strain dynamic impact coefficient of each measuring point is analysed, as shown in Tables 6 and 7. Only the three conditions of the bridge deck are good, medium, and poor.

A comparison of Tables 6 and 7 shows the following findings: (1) When the condition of the bridge deck is good, the difference between the strain dynamic impact coefficients of the two driving modes is small, but as the condition of the bridge deck deteriorates, the gap gradually increases. (2) In the case of a poor bridge deck, the eccentric load impact coefficient at point 3 is approximately 68% higher than the intermediate load impact coefficient. (3) When the bridge deck is in good condition and under the effect of partial load and medium load, the dynamic impact coefficients of measuring point 1 (cantilever plate), measuring point 5 (top plate centre), and measuring point 9 (bottom plate centre) are similar, and in other parts, the midload impact coefficient is less than the eccentric load impact coefficient. (4) Comparing the dynamic impact coefficient (0.177) calculated by current Chinese codes, the strain dynamic impact coefficient is higher than approximately 69% when the bridge deck condition is normal.

The current general code for bridge and culvert design in China stipulates that the dynamic impact coefficient is 0.3 when performing local check calculations on T-beam and box beam cantilever plates. As shown in Tables 6 and 7, under acceptable bridge deck conditions, the longitudinal

Table 6: Strain dynamic impact coefficient of each measuring point of the composite box girder when $L = 5.8$ m.

Measuring point	Good	Normal	Poor
1	0.113	0.324	0.441
2	0.102	0.303	0.398
3	0.106	0.308	0.402
4	0.106	0.310	0.404
5	0.124	0.320	0.435
6	0.107	0.305	0.434
7	0.112	0.317	0.441
8	0.118	0.328	0.447
9	0.124	0.335	0.435

Table 7: Strain dynamic impact coefficient of each measuring point of the composite box girder when $L = 1.0$ m.

Measuring point	Good	Normal	Poor
1	0.111	0.324	0.597
2	0.122	0.326	0.611
3	0.131	0.353	0.674
4	0.135	0.361	0.735
5	0.128	0.334	0.633
6	0.117	0.336	0.623
7	0.119	0.335	0.634
8	0.122	0.336	0.661
9	0.123	0.337	0.652

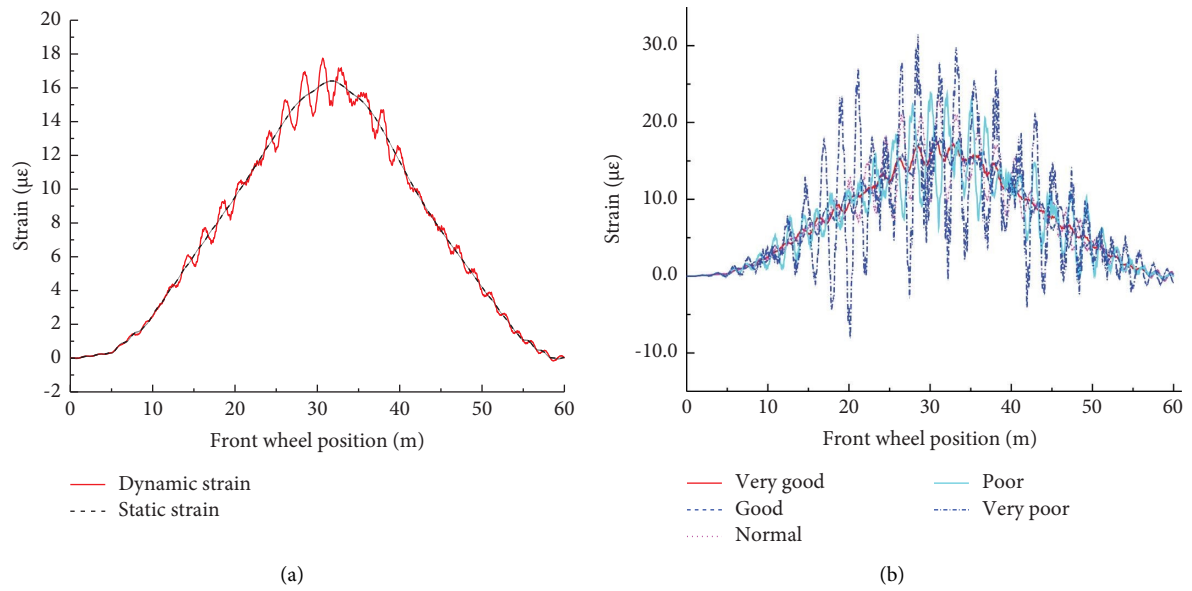

Figure 8: Longitudinal normal strain time history curve under different bridge deck conditions: (a) typical longitudinal normal strain time history curve and (b) longitudinal normal strain time history curve under different bridge deck conditions.

normal strain does not exceed the standard value, but when the bridge deck condition is poor, the coefficient obviously exceeds the specification value. The transverse stress of the combined box beam cantilever plate, especially the transverse normal stress at the root of the cantilever plate, is an important part of its local check. Therefore, still taking the 50 m simple-supported composite box girder as an example to analyse the transverse stress impact coefficient of the cantilever plate root, the model is a three-axle vehicle with a lateral L = 2.8 m and a speed of 5 m/s. The bridge deck condition is good, the tension is positive, and the compression is negative. Figure 9 shows the transverse normal strain time-history curve of the cantilever plate root at the midspan of the composite box girder with corrugated steel webs.

The lateral normal strain time history curve of Figure 9 shows that when the vehicle crosses the bridge, the transverse normal strain at the root of the cantilever plate will have multiple peaks and troughs. When the front axle of the vehicle reaches the position near the midspan, the maximum tensile stress occurs. When the middle axis reaches the midspan (the front axis is approximately 34 m), the second

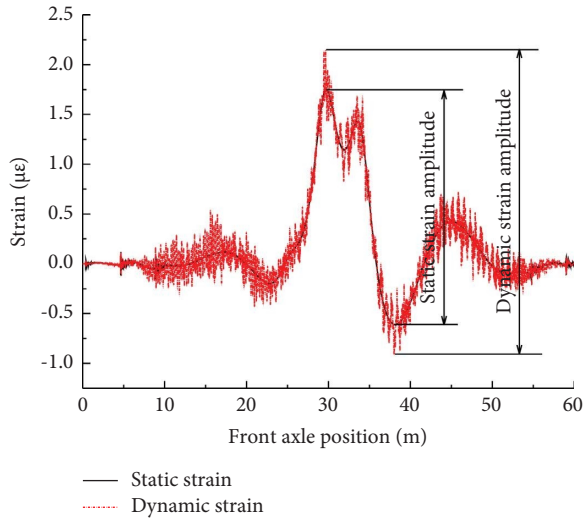

Figure 9: Typical lateral normal strain time history curve of the cantilever plate root.

Table 8: Transverse strain dynamic impact coefficient of the cantilever plate root of a 50 m simply supported composite box girder.

Measuring point	Lateral strain	Good	Normal	Poor
1	Tensile strain	0.212	0.471	1.357
	Compressive strain	0.637	1.370	4.552
2	Tensile strain	0.219	0.489	1.390
	Compressive strain	0.613	1.307	4.329

peak tensile stress appears. When the rear axle reaches the midspan (the front axle is approximately 38.5 m), the maximum compressive stress occurs. The static stress amplitude and dynamic stress amplitude in the figure are quite different, but these phenomena have an important effect on the fatigue stress amplitude of the transverse reinforcement of the composite box girder and the shear fatigue stress amplitude of the corrugated steel web. Therefore, the lateral dynamic impact coefficient of the cantilever plate root should be clarified.

To analyse the dynamic impact coefficient of the transverse normal strain of the cantilever plate root of the composite box girder, two measuring points (3.2 m and 3.0 m from the edge of the cantilever plate) of the midsection cantilever plate of the 50 m simply supported composite box girder were selected to calculate the transverse normal strain dynamic impact coefficient, as shown in Table 8.

A comparison of Tables 7 and 8, under the same bridge deck conditions, reveals that the transverse strain impact coefficient is greater than the longitudinal strain impact coefficient. When the composite box girder is locally checked and the bridge deck is in good condition, its average transverse strain impact coefficient also reaches 0.42. However, the coefficient given in the current Chinese codes is only 0.3, and the impact coefficient is greater in other bridge deck conditions. As the impact coefficient has an important effect on the calculation of the fatigue stress amplitude of the transverse reinforcement of the cantilever plate of the combined box girder and the fatigue stress amplitude of the corrugated steel webs under shear, special attention should be given to it.

4.3. Impact Analysis of Vehicle Condition. According to domestic and international codes, the dynamic impact coefficient of the bridge is related to the number of axles and vehicle speeds. To analyse the influence of vehicle factors on the dynamic impact coefficient of the composite box girder with corrugated steel webs, the 30 m simply supported composite box girder with corrugated steel webs of sample 1 was selected, and the deflection dynamic impact coefficient of each measuring point for different axle vehicle loads and different vehicle speeds (7.6 km/h–93.6 km/h) was calculated. The results are shown in Figures 10–12. Both types of vehicles use the same bridge deck conditions, acting on the bridge deck's lateral position L = 3.4 m. The shading in the figure indicates the deflection impact coefficient of the composited box girder analysed in accordance with our country's current codes, the dot-dashed line indicates the limit dynamic impact coefficient analysed according to AASHTO, and 1-7 represent the measurement points shown in Figure 3(b).

Figures 10–12 show that the dynamic shock coefficient calculated by using the US code is greater than the calculation results of the Chinese code. A comparison and analysis of the dynamic impact coefficient of each measuring point reveals that the quality of the bridge deck and the vehicle model and speed will affect the impact coefficient. As the condition of the bridge deck changes from good to poor, the dynamic impact coefficient of each measuring point gradually increases. When the condition of the bridge deck is good, the dynamic impact coefficient of each measuring point is less than the national standard value, and when the condition of the bridge deck is normal, the dynamic impact coefficient of most of the measuring points is greater than the national standard value. When the condition of the bridge deck is poor, the dynamic impact coefficients of almost all the measuring points are greater than the national norms. With an increase in vehicle speed, the dynamic shock coefficient shows a trend of increasing-decreasing-increasing-decreasing, but the specific change range exhibited by different vehicle types is different. For two-axle vehicles, the speed range with a large impact coefficient is between 20 km/h and 50 km/h; for three-axle vehicles, the speed range with a large impact coefficient is between 60 km/h and 80 km/h. To further illustrate the impact of different vehicle types on the impact coefficient, the average value of the dynamic impact coefficient of each measurement point at different vehicle speeds is shown in Figure 13. As the condition of the bridge deck changes from good to poor, the dynamic impact coefficient gradually increases. Under the same conditions and speed of the bridge deck, if the vehicle type is different, the dynamic impact coefficient is different. With increasing speed, the dynamic shock coefficient has changed from being larger for two-axle models than three-axis models to being larger for three-axis models than two-axis models.

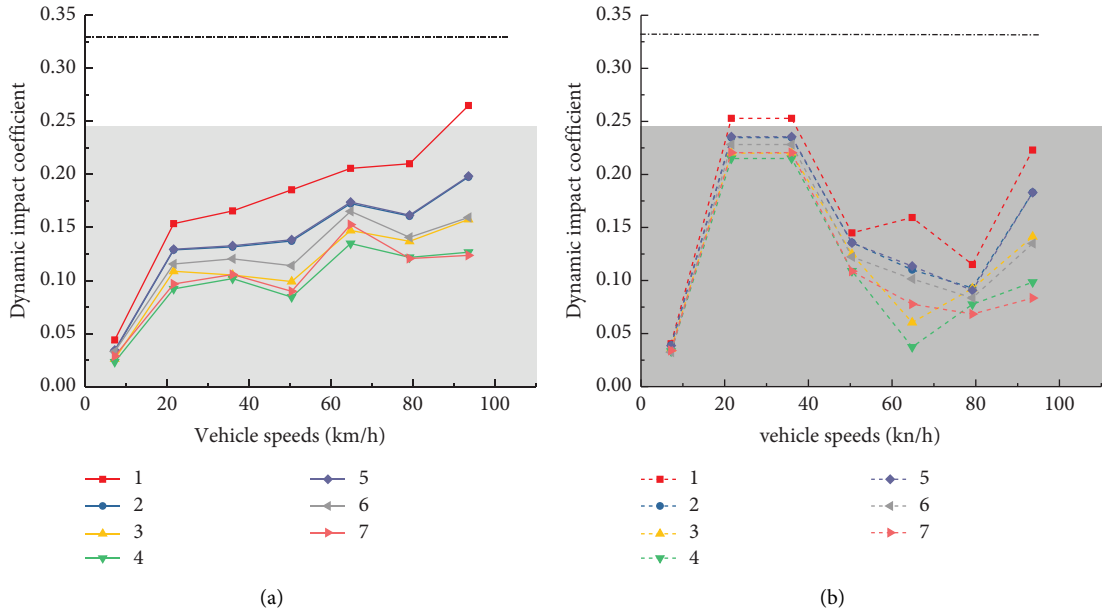

Figure 10: Coefficient of dynamic shock when bridge deck is good. (a) Three-axis models. (b) Two-axis models.

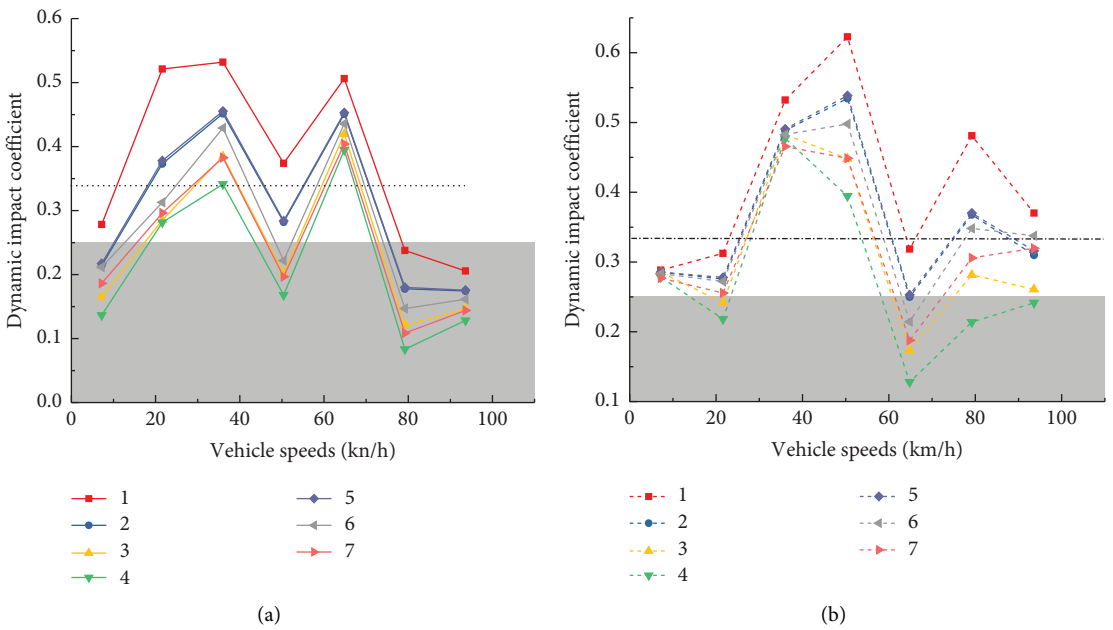

Figure 11: Coefficient of dynamic shock when bridge deck is medium. (a) Three-axis models. (b) Two-axis models.

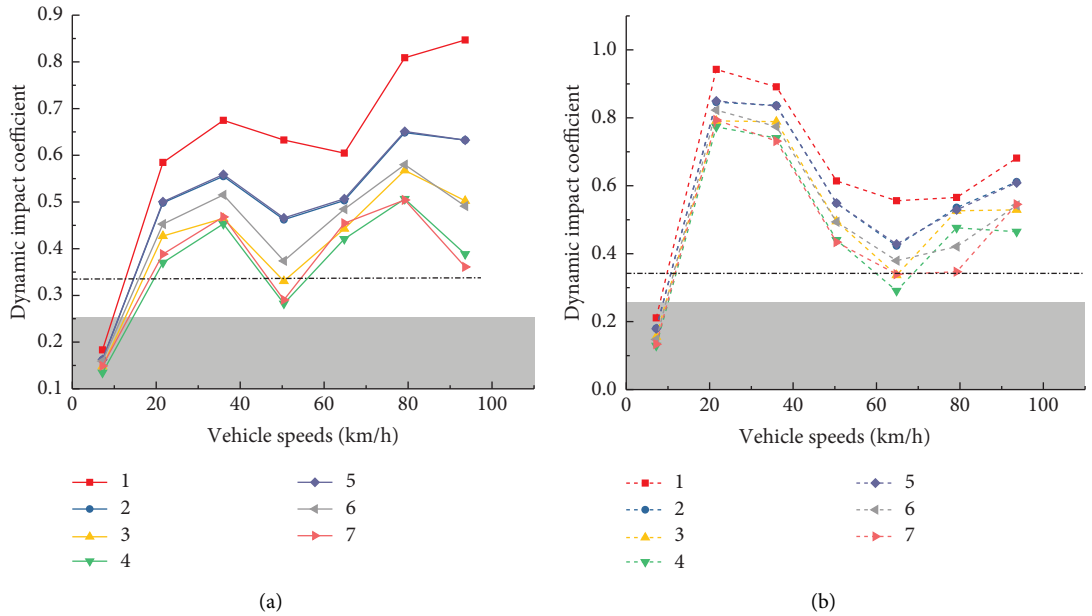

Figure 12: Coefficient of dynamic shock when bridge deck is poor (a) Three-axis models. (b)Two-axis models.

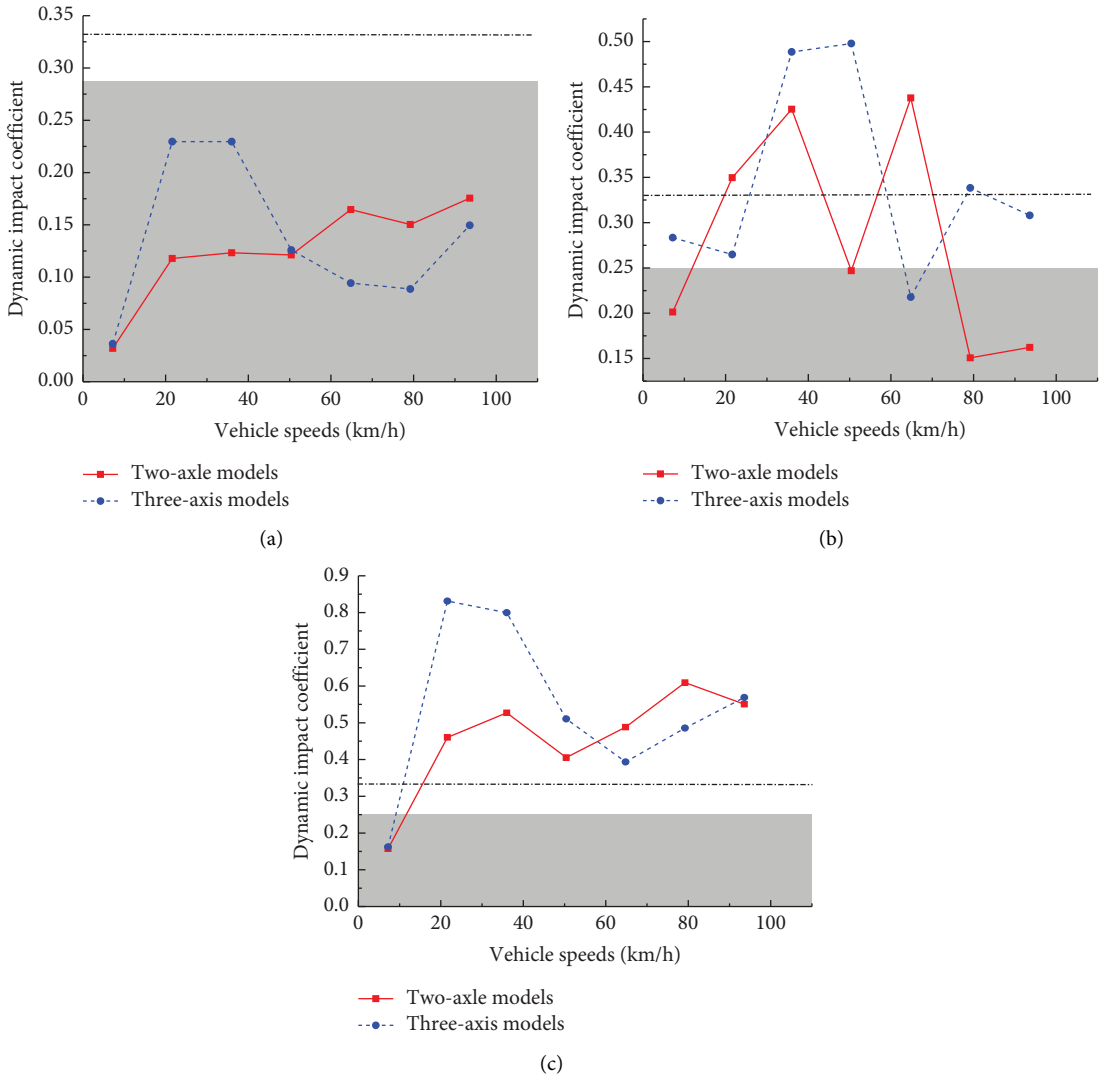

Figure 13: Comparison of the mean value of the dynamic shock coefficient of two types of vehicles. (a) Good bridge deck. (b) Normal bridge deck. (c) Poor bridge deck.

5. Conclusion

By an investigation of the dynamic response of composite box girder bridges with corrugated steel webs, the following conclusions are drawn:

(1) When the composite box girder with corrugated steel webs is replaced with an ordinary concrete web with equal wave height, the difference between the low-order deflection natural frequencies of the two box girders is small. However, the difference between them will increase as the frequency order increases, and the frequency of the composite box girder with corrugated steel webs is lower than that of the corresponding concrete box girder. The comparison results of the deflection impact coefficients of the two types of box girder show that when the bridge deck is in good condition, the gap between the two results is small, and when the bridge deck is in poor condition, the dynamic impact coefficient of the composite box girder is much larger than that of the concrete box girder.

(2) A comparison of various factors that affect the flexural dynamic impact coefficient of the composite box girder reveal that the quality of the bridge deck has the most obvious impact on the dynamic response. According to a comparison of the refined vehicle-bridge coupling vibration analysis results, the calculation methods of the impact coefficient in most domestic and international bridge codes are only applicable to the situation where the bridge deck condition is good or better.

(3) Unlike the dynamic impact coefficient of deflection, the local characteristics of the dynamic impact coefficient of strain are relatively obvious, and when a vehicle is driven under the conditions of intermediate load and partial load, the gap between two strain impact coefficients of some measurement points is large. When the combined box girder is locally checked and the bridge deck is in good condition, its average transverse strain impact coefficient also reaches 0.42. However, the coefficient given in our country's current codes is only 0.3, and the impact coefficient is greater in other bridge deck conditions. Thus, special attention should be given to the design.

(4) The quality of the bridge deck and the vehicle model and speed will affect the impact coefficient. As the bridge deck changes from good to poor, the dynamic impact coefficient gradually increases. With increasing vehicle speed, the dynamic shock coefficient shows a trend of increasing-decreasing-increasing-decreasing, but the specific change range exhibited by different vehicle types is different. For two-axle vehicles, the speed range with a large impact coefficient is between 20 km/h and 50 km/h. For three-axle vehicles, the speed range with a large impact coefficient is between 60 km/h and 80 km/h. With increasing speed, the dynamic shock coefficient has changed from being larger for two-axle models larger than three-axis models to being larger for three-axis models than two-axis models.

Data Availability

The data used to support the findings of this study are included within the article.

Conflicts of Interest

The authors declare that they have no conflicts of interest.

Acknowledgments

This study was supported partially by the National Natural Science Foundation of China (Grant no. 52268027) and Si chuan Natural Science Foundation Project (2022NSFSC0427).

References

[1] Z. Zhang, G. Wang, and F. Jiang, "Natural vibration characteristics of continuous box composite girder with corrugated steel webs of uniform cross-section," *China Railway Science*, vol. 42, no. 4, pp. 51–59, 2021.

[2] S. Chen, C. Zhang, and G. Shuirong, "An experimental study on dynamic characteristics of a single-box multi-cell composite girder bridge with corrugated steel webs," *Journal of Vibration and Shock*, vol. 36, no. 12, pp. 122–127, 2017.

[3] S. Zheng, S. Wan, and H. Cheng, "Research on the dynamic characteristics of multi—room single box composite girder with corrugated steel webs," *Journal of Railway Engineering Society*, vol. 34, no. 9, pp. 41–46, 2017.

[4] S. Zheng, K. Hu, and H. Cheng, "Analysis on influence of externally prestressed tendons on fundamental frequency of continuous box girder with corrugated steel webs," *Journal of Railway Engineering Society*, vol. 38, no. 5, pp. 53–59, 2021.

[5] W. Wang, D. Zhai, Y. Bai et al., "Loss of QKI in macrophage aggravates inflammatory bowel disease through amplified ROS signaling and microbiota disproportion," *Cell death discovery*, vol. 7, no. 1, pp. 58–65, 2021.

[6] J. Wei, L. Deng, and W. He, "Vehicle-bridge coupled vibration analysis and calculation of dynamic impact factor for the PC box-girder bridge with corrugated steel webs," *Journal of Vibration Engineering*, vol. 29, no. 6, pp. 1041–1047, 2016.

[7] J. Wei, L. Deng, and W. He, "Local and global impact factors analysis for PC box girder bridges with corrugated steel webs," *Vibration and Shock*, vol. 36, no. 8, pp. 22–28, 2017.

[8] *JTG D60-2015 General Specification for Design of Highway Bridges and Culverts*, People's Communications Press Co. Ltd, Beijing, China, 2015.

[9] L. Li, *Flexural Mechanical Properties and Experimental Study of Corrugated Steel Web Composite Box Girders Considering Shear Deformation*, Doctoral dissertation of Lanzhou Jiaotong University, Gansu, China, 2019.

[10] L. Deng and W. Wang, "Research progress of highway bridge dynamic impact coefficient," *Journal of Dynamics and Control*, vol. 14, no. 4, pp. 289–300, 2016.

[11] L. Deng, W. He, and F. Wang, "Dynamic impact factors for simply supported bridges with different cross-section types," *Vibration and Shock*, vol. 34, no. 14, pp. 70–75, 2015.
[12] L. Deng, W. Wang, and X. He, "Optimization and application of fatigue design based on AASHTO code," *Journal of China Highway and Transport*, vol. 30, no. 3, pp. 40–48, 2017.
[13] American Association of State Highway and Transportation Officials, *Standard Specifications for Highway Bridges*, Aashto, Washington, DC, USA, 1992.
[14] American Association of State Highway and Transportation Officials (Aashto), *AASHTO LRFD Bridge Design Specifications 6thed*, AAASHTO, Washington, DC, USA, 2012.
[15] Japan Road Association, *Specifications for Highway Bridges, Part 1*, Common Specifications, Tokyo, Japan, 1996.
[16] Ontario Ministry of Transportation and Communications, *Ontariohighway Bridge Design Code*, Toronto, Ontario, Canada, 1983.
[17] Ontario Ministry of Transportation and Communications, *Ontariohighway Bridge Design Code*, Toronto, Ontario, Canada, 1991.
[18] M. Zhou, Y. Zhang, and L. Li, "Research on bending vibration frequency of thin-walled simply supported box girder," *Highway Transportation Science and Technology*, vol. 35, no. 1, pp. 72–78, 2018.
[19] Ministry of Communications of the People's Republic of China, *JTJ 021-89 General Specification for Design of Highway Bridges and Culverts*, People's Communications Press, Beijing, China, 1989.
[20] L. Deng and C. S. Cai, "Identification of parameters of vehicles moving on bridges," *Engineering Structures*, vol. 31, no. 10, pp. 2474–2485, 2009.
[21] X. F. Yin, Z. Fang, C. S. Cai, and L. Deng, "Non-stationary random vibration of bridges under vehicles with variable speed," *Engineering Structures*, vol. 32, no. 8, pp. 2166–2174, 2010.
[22] L. Deng, *System Identification of Bridge and Vehicle Based on Their Coupled vibration*, Louisiana State University, Baton Rouge, LA, USA, 2009.
[23] X. Li, L. Zhang, and J. Zhang, "State-of-the-art review and trend of studies on coupling vibration for vehicle and highway bridge system," *Engineering Mechanics*, vol. 25, no. 03, pp. 230–240, 2008.